BRDF Effects in Satellite Retrieval of Surface Spectral Reflectance in Solar Spectral Region

A. P. Trischenko, Z. Li, W. Park, and J. Cihlar
Canada Centre for Remote Sensing
Ottawa, ONT, K1A 0Y7, Canada

Introduction

Surface reflectance/albedo is important for many geophysical applications, atmospheric circulation, and climate modeling (Henderson-Sellers et al. 1993). It is a key input parameter for land type classification and serves as a major boundary condition in surface-atmosphere radiative transfer modeling, which determines the distribution of solar energy between the surface and the atmosphere. Surface reflective properties can be retrieved from satellite observations. A surface target may be observed by satellite from different viewing directions. Due to the anisotropy of surface reflection, this leads to diversity of surface properties retrieved from satellite composite images (Li et al. 1996). To address this problem, one needs to determine the surface bidirectional reflectance distribution function (BRDF) properties and correct for them in the final product. Integrals of BRDF functions result in the so-called black-sky and white-sky albedos that convey important information concerning the inherent properties of surface albedo (Wanner et al. 1997).

To provide the science teams of the Atmospheric Radiation Measurement (ARM) Program and other interested users with necessary information to characterize surface radiative properties, we processed data from the advanced very high resolution radiometer (AVHRR) onboard the National Oceanic and Atmospheric Administration (NOAA)-14 satellite for the 1998–1999 period, with work in progress for 2000. The retrievals were done for the Southern Great Planes (SGP) and North Slope of Alaska (NSA) ARM regions as well as Mackenzie Global Energy and Water Experiment (GEWEX) Study (MAGS) area (Stokes and Schwartz 1994; Stewart et al. 1998). A new version of the Geocoding and Compositing System (GEOCOMP-N), as implemented at the Canada Centre for Remote Sensing (CCRS), has been used to create clear-sky composite images from AVHRR imagery.

A parameterized version of the 5S radiative transfer code called SMAC was applied for atmospheric correction (Rahman and Dedieu 1994). The parameters of the kernel-driven BRDF model of Roujean et al. (1992) were derived following a LSE fitting procedure (Li et al. 1996). Over complex terrain, a pixel containing an inclined surface has an effective geometry of observation different from that for a flat horizontal pixel. As a result, a special correction is required to account for the effect of surface topography (Vermote et al. 1997a; Richter 1998). The main task for this correction is to eliminate the influence of pixel orientation, i.e., to have the retrievals independent of pixel orientation. To this end, modifications were made to the SMAC algorithm for correcting the topographic effect of satellite imagery.

Finally, we studied the coupling between surface BRDF properties and atmospheric radiation due to multiple scattering, which may impede the accuracy of surface reflectance retrievals under certain conditions (Lee and Kaufman 1986). Uncertainties in the retrieval of surface reflectance around the ARM Central Facility site in the SGP area are estimated. It is found that use of a Lambertian assumption (ignoring the BRDF) in the retrieval leads to uncertainty that correlates with atmospheric opacity and the geometry of observation and may be as high as 15% to 20% under certain conditions.

AVHRR Data Processing

All daytime AVHRR/NOAA-14 orbital data, acquired by the CCRS satellite receiving station located at Prince Albert, Saskatchewan, Canada, were processed. The satellite imagery encompasses the bulk area of Canada and the U.S. continent. Data processing was done with the GEOCOMP-N system that performs clear-sky compositing (10-day), resampling, calibration, atmospheric correction, and BRDF correction, etc. SGP and NSA/MAGS regions were covered every day during the warm season. An atmospheric correction was applied only to clear-sky composite pixels having different observation geometries defined by sun zenith angle (SZA [θ_0]), viewing zenith angle (VZA [θ]), and relative azimuth angle (RAA [ϕ]). To unveil the true spatial variation of surface reflectivity, surface reflectance resulting from the atmospheric correction were normalised to a common geometry ($\theta_0 = 45^0$, $\theta^0 = 0$, $\phi = 0^0$) with a knowledge of the surface BRDF

$$\rho(\theta_0 = 45^0, \theta = 0, \phi = 0) = \rho(\theta_0, \theta, \phi)\Omega(\theta_0 = 45^0, \theta = 0, \phi = 0) / \Omega(\theta_0, \theta, \phi) \quad (1)$$

where $\Omega(\theta_0,\theta_v,\phi)$ is the kernel-driven BRDF model proposed by Roujean et al. (1992)

$$\Omega(\theta_0, \theta_v, \phi) = 1 + K_1/K_0 * f_1(\theta_0, \theta_v, \phi) + K_2/K_0 * f_2(\theta_0, \theta_v, \phi) \quad (2)$$

Coefficients in Equation 2 were obtained by the LSE method for each of the 24 surface types classified by the USG (urban, cropland, grassland, etc.). To account for seasonal changes, the coefficients were derived for different bins of the Normalised Difference Vegetation Index (NDVI) ($\Delta_{NDVI} = 0.2$) (Li et al. 1996). Examples of surface type distribution for SGP and NSA/MAGS regions are presented in Figure 1a-b. BRDF-corrected images for the SGP area are shown in Figure 2 for the two solar channels of AVHRR/ NOAA-14 during the period August 11-20, 1998. Corresponding images for NSA/MAGS regions are shown in Figure 3.

Method for Surface Topography Correction of AVHRR Images

Due to the scattering and reflection of solar radiation in the surface-atmosphere system, atmospheric correction of satellite measurements is coupled to the topography of a pixel and its surrounding area (Proy et al. 1989; Vermote et al. 1997a; Richter 1998). Two surface features play major roles in determining apparent radiance at the top-of-the-atmosphere (TOA): 1) surface inclination and 2) obstruction of the sky dome by surrounding rugged relief. Surface inclination changes the geometry of reflection and thus it effectively modifies the three angles between the sun, satellite, and target. The second factor alters the amount of diffuse radiation, creates shadow(s) by blocking the direct solar beam,

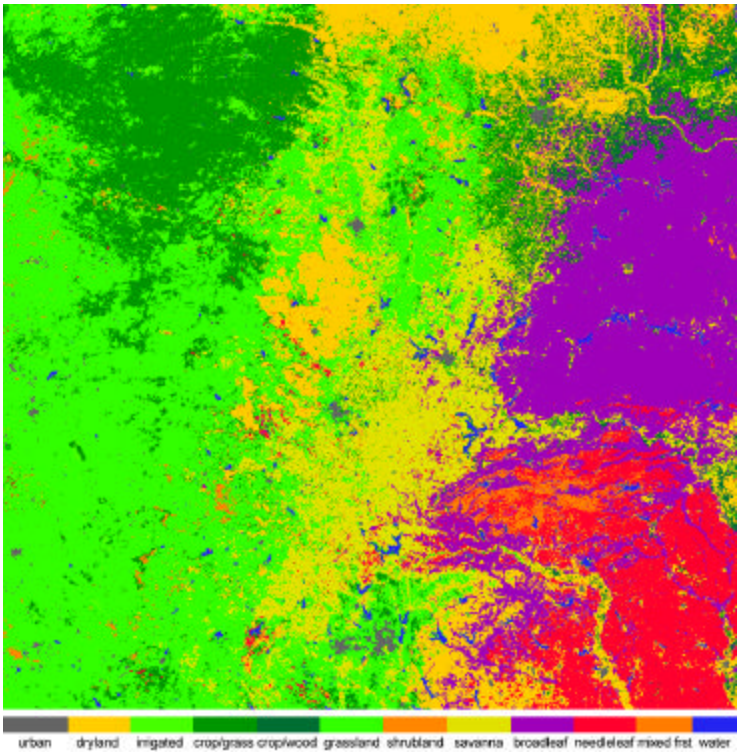

Figure 1a. Surface type distribution around SGP site according to USGS classification.

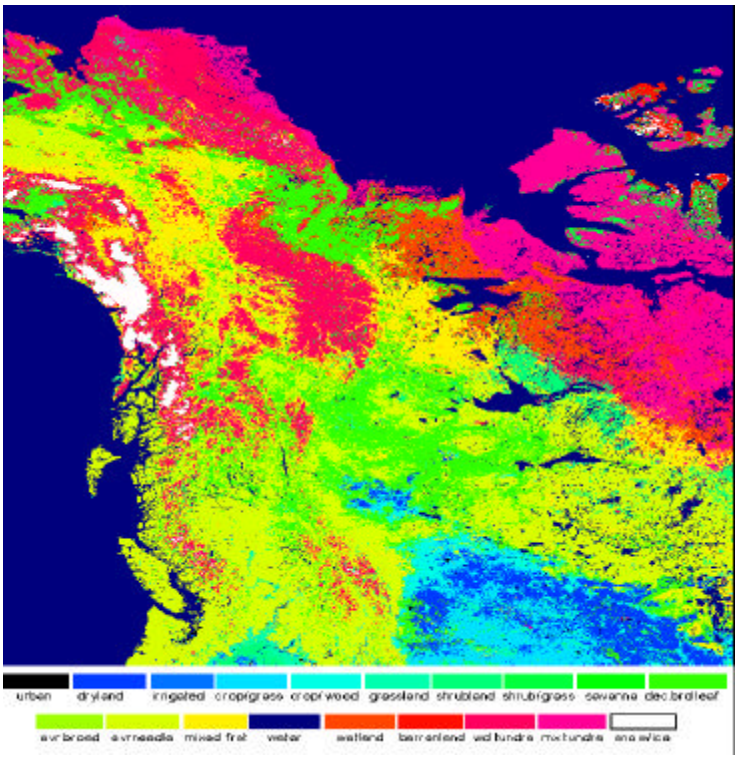

Figure 1b. Surface type distribution in NSA/MAGS region according to USGS classification.

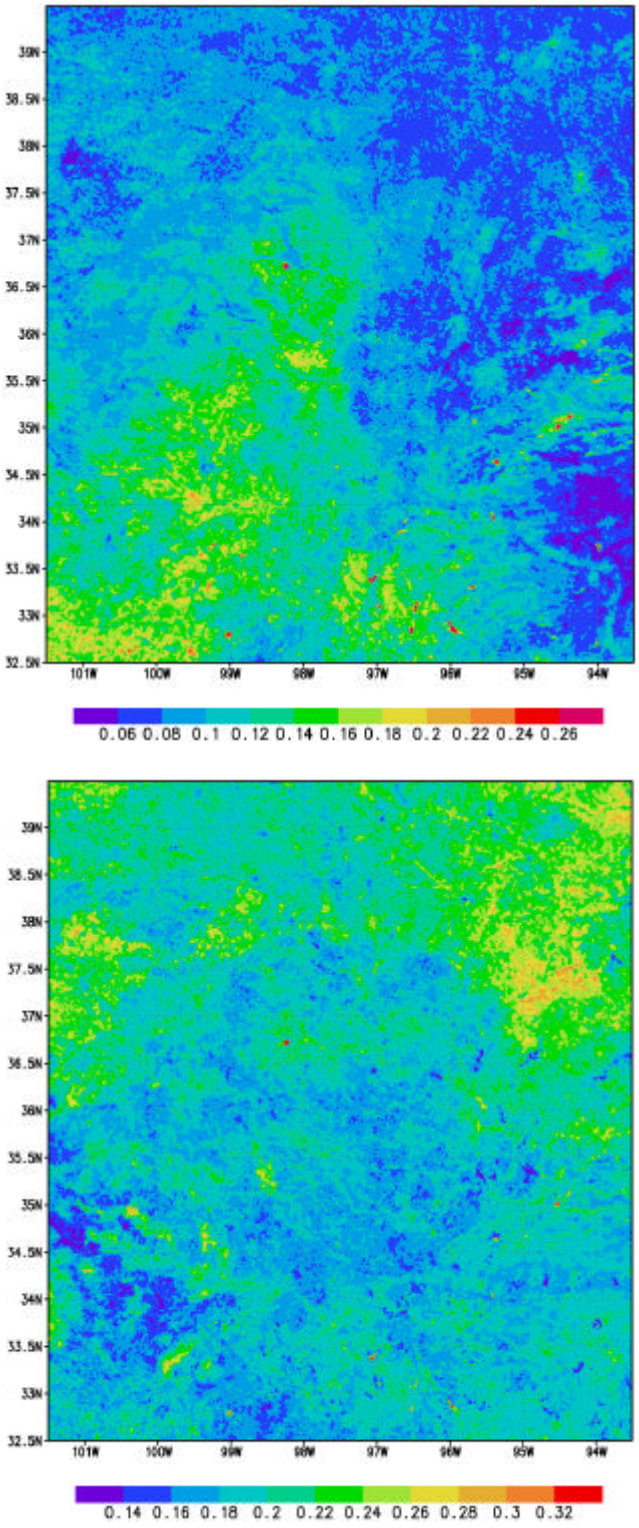

Figure 2. BRDF-corrected surface reflectances in channel 1 (0.63μm) and channel 2 (0.85μm) AVHRR for ARM SGP area for August 11-20, 1998.

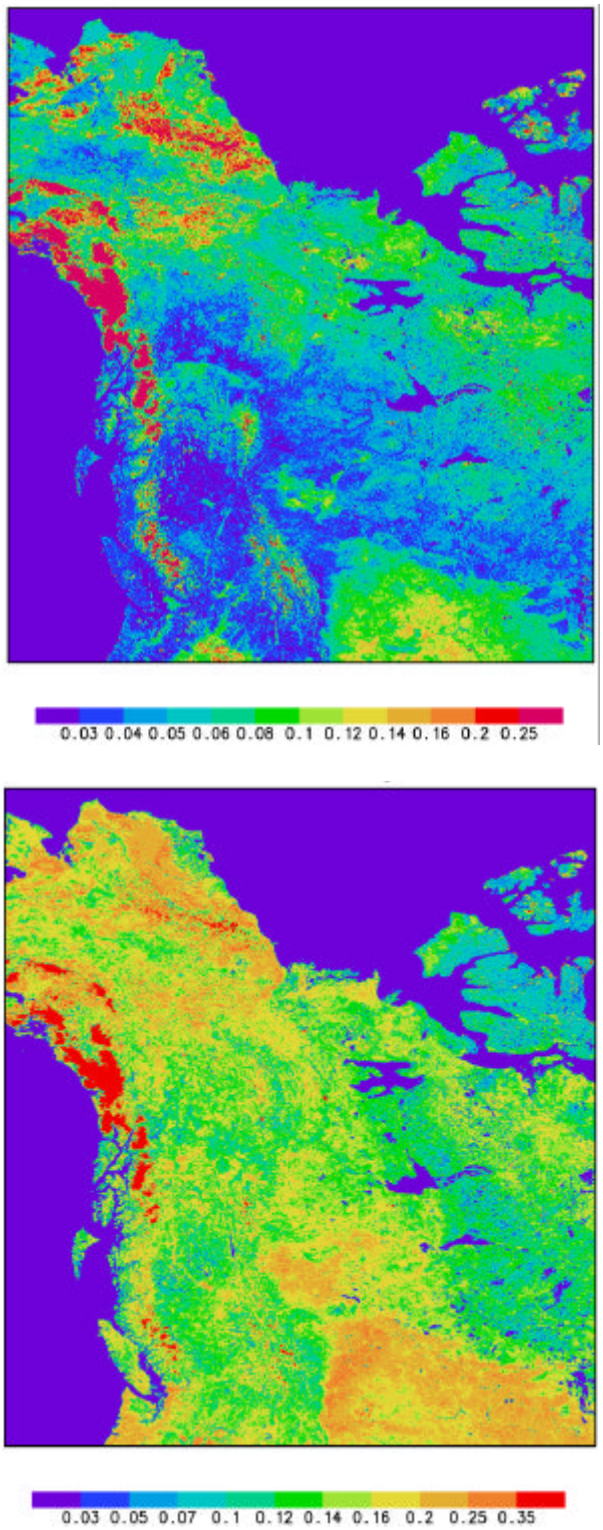

Figure 3. BRDF-corrected surface reflectances in channel 1 (0.63µm) and channel 2 (0.85µm) AVHRR for ARM NSA /MAGS region for August 1-11, 1998.

and produces reflection from the neighbouring area. For a non-Lambertian surface, the BRDF effect differs from that over a flat surface. The following describes formulae modifying the SMAC algorithm to account for the effect of an inclined surface in atmospheric correction.

Let us denote the slope of a pixel as β, and the aspect angle as γ (relative to the North direction), and use superscript * to denote parameters for an inclined surface. The zenith angles θ_0^* and θ^* for an inclined surface relative to its normal (Iqball 1983) are

$$\begin{aligned} \cos\theta_0^* &= \cos\beta\cos\theta_0 + \sin\beta\sin\theta_0\cos(\gamma-\phi_s), \\ \cos\theta^* &= \cos\beta\cos\theta + \sin\beta\sin\theta\cos(\gamma-\phi) \end{aligned} \tag{3}$$

The global downward radiation G at the surface consists of two parts: the direct beam B and diffuse radiation D: G = B + D. The correction due to surface inclination for the direct component is straightforward

$$B^* = B_0\cos\theta_0^*\Theta(90-\theta_0^*) = (B/\cos\theta_0)\cos\theta_0^*\Theta(90-\theta_0^*) = B\,r_b\Theta(\cos\theta_0^*) \tag{4}$$

where $r_b = \cos\theta_0^*/\cos\theta_0$, B_0 is the direct radiation for normal incidence, B is the direct radiation for the horizontal surface, B* is the direct radiation for inclined surface, and $\Theta(x) = \Theta(90 - \theta_0^*) = \Theta(\cos\theta_0^*)$ is the Heaviside function, equal to 1 for a positive argument and 0 for a negative argument. It is used here to obtain zero radiation for a shadowed pixel.

The topographic effect on diffuse radiation includes possible blocking of the sun, obscuring part of horizon, and reflection from the surrounding area. Following Hay (1985) and Richter (1998), the effect is taken into account by the following formula

$$D^* = D\{\Theta(\mu_0^*)t_s(\theta_0)r_b + [1-\Theta(\mu_0^*)\,t_s(\theta_0)]V_{sky}\} + \rho_e G/\pi(1-V_{sky}) \tag{5}$$

where μ_0^* is $\cos\theta_0^*$, $t_s(\theta_0)$is atmospheric transmittance for direct radiation, ρ_e is reflectance of the surrounding area, and V_{sky} is the so-called configuration or sky-view factor (proportional to the solid angle corresponding to the non-obscured portion of the sky dome).

Due to limited knowledge of elevation h and for the sake of computational efficiency, we use a simple parameterization for V_{sky} proposed by Kondratyev (1977)

$$V_{sky} = 1/2\,(1+\cos\beta) \tag{6}$$

Therefore, total radiation on an inclined surface G* is approximated by

$$G^* = B^* + D^* = Br_b\,\Theta(\mu_0^*) + [D\{\Theta(\mu_0^*)\,t_s(\theta_0)\,r_b + [1-\Theta(\mu_0^*)\,t_s(\theta_0)]V_{sky}\} + \rho_e G/\pi(1-V_{sky})] \tag{7}$$

The basic equation used in SMAC for retrieval of surface Lambertian reflectance from TOA apparent reflectance in the case of a "flat" pixel is

$$\rho_T(\theta_0,\theta,\phi) = \rho_a(\theta_0,\theta,\phi) + [t_s(\theta_0) + t_d(\theta_0)][\rho_p t_v(\theta) + \rho_e t_d(\theta)]/(1-\rho_e S) \quad (8)$$

where ρ_T is the TOA spectral reflectance measured by satellite, ρ_a is the atmospheric reflectance; $T(\theta) = t_s(\theta) + t_d(\theta)$ is the total transmittance consisting of direct $t_s(\theta)$ and diffuse $t_d(\theta)$ transmittances; ρ_p is the surface pixel reflectance; ρ_e is the average reflectance of the pixel and surrounding area (reflecting towards the sensor's field of view [FOV]), and S is the spherical albedo of the atmosphere. SMAC provides parameterizations for computing these components upon atmospheric constituents.

Per the definition of direct and diffuse transmittances,

$$t_s = Bs/S_0\mu_0 ; t_d = D_s/S_0\mu_0 \quad (9)$$

one can transform Equation 8 into the following expression

$$\rho_T = \rho_a + \rho_p (B_s/S_0\mu_0 + D_s/S_0\mu_0)\, t_v(\theta)/(1-\rho_e S) + \rho_e (B_s/S_0\mu_0 + D_s/S_0\mu_0) t_d(\theta)/(1-\rho_e S) \quad (10)$$

where B_s and D_s are direct and diffuse components of downwelling irradiance at the surface level.

To account for the surface topography effects described above, the term $B_s/S_0\mu_0$ should be changed to $B_s*/S_0\mu_0$, and $D_s/S_0\mu_0$ to $D_s*/S_0\mu_0$. In case of $\rho_p = \rho_e = \rho$, Equation 10 becomes

$$\begin{aligned}\rho_T(\theta_0,\theta,\phi) = {} & \rho_a(\theta_0,\theta,\phi) + \rho\,[t_v(\theta) + t_d(\theta)][t_s(\theta_0)\, r_b \Theta(\mu_0*) + t_d(\theta_0)\{\Theta(\mu_0*)\, t_s(\theta_0)\, r_b \\ & + [1-\Theta(\mu_0*)\, t_s(\theta_0)]\quad V_{sky} + \\ & (t_s\theta_0 + t_d(\theta_0))\rho/\pi(1-V_{sky})\}]/1-\rho\, S)\end{aligned} \quad (11)$$

Expression 11 and its inverted form may be used in the retrieval of surface reflectance ρ from AVHRR measured apparent reflectance ρ_T in the case of an inclined surface. A sensitivity study conducted with Equation 11 showed an improved quality of the images, where surface reflectance maps in mountainous regions were smoother due to the correction of the radiation field for the effect of an inclined surface. Angles modified according to Equation 3 should be used in fitting the BRDF shape and correcting surface reflectance maps.

BRDF Effect in the Retrieval of Surface Reflectance

Often, retrieval algorithms are concerned only with the removal of atmospheric attenuation due to molecular, gaseous, and aerosol scattering, and absorption. However, there is an interaction between the surface and the atmosphere, as a result of multiple scattering, that is affected by surface BRDF properties. This could impact the accuracy of surface reflectance retrievals under certain conditions

(Lee and Kaufman 1986). For satellite data with high spatial resolution, like Landsat TM or SPOT HRV data, multiple scattering makes the pixel adjacency effect also important, although for data with a pixel size larger than 1 km, this effect is much less significant (Vermote et al. 1997b).

The coupling between surface anisotropy properties and radiation means that for accurate atmospheric correction, we need to have a priori knowledge of the BRDF function for a given pixel (Vermote et al. 1997b). As such, the retrieval in the case of strong BRDF effects should be done iteratively (Wanner et al. 1997). To evaluate the impact of the BRDF, surface and TOA reflectances were simulated with the 6S code (Vermote et al. 1997a) using typical BRDF models derived around the ARM Southern Great Plains Central Facility (SGP CF) site (mixed dryland, cropland, and pasture). Model parameters K_0, K_1, K_2 are 0.134, 0.022, 0.182 for channel 1, and 0.227, 0.039, 0.361 for channel 2. They are compared to the results obtained by neglecting BRDF properties. Figures 4 and 5 present results for principal and perpendicular plane geometry in channels 1 and 2, respectively. A continental aerosol model was assumed with $\tau_{0.55\mu m} = 0.07$, typical of clear-sky conditions in that region. Atmospheric profiles were based on the US62 atmosphere. These computations show that neglecting BRDF properties in the satellite retrieval of surface reflectance generally leads to relative errors less than 5%. Uncertainty becomes larger (up to 15% to 20%) for SZA and VZA > 60° and more turbid aerosol conditions.

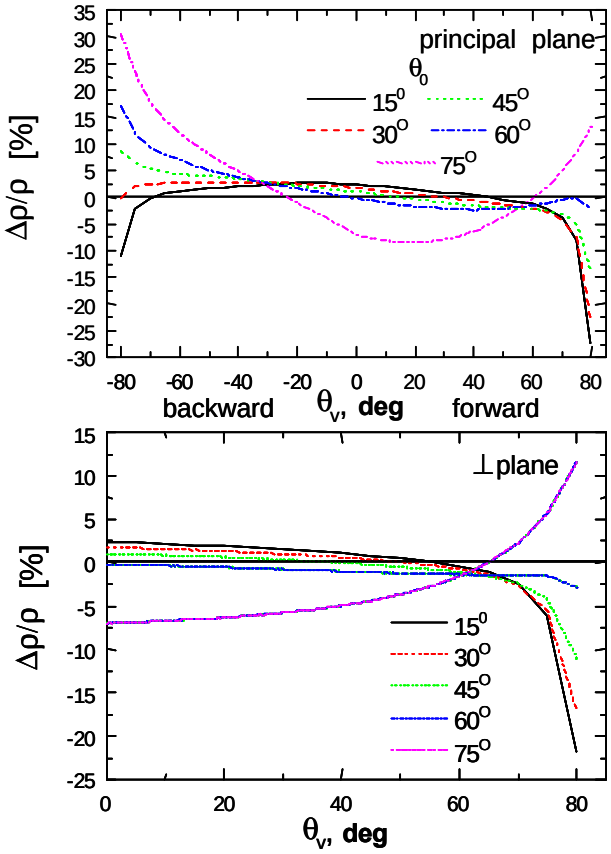

Figure 4. Uncertainty of Lambertian assumption in retrieval of surface reflectance in AVHRR channel 1 (0.63μm) for SGP CF site area.

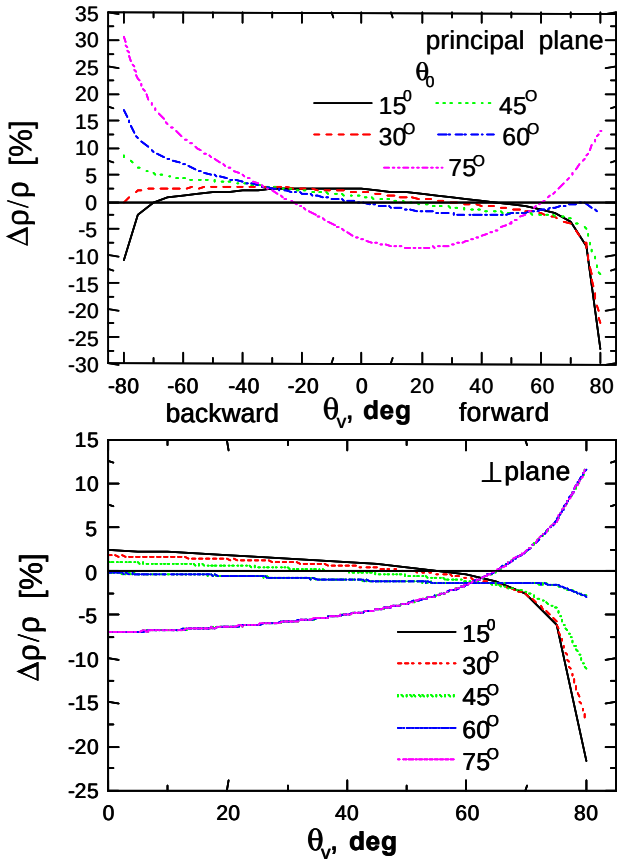

Figure 5. Uncertainty of Lambertian assumption in retrieval of surface reflectance in AVHRR channel 2 (0.85μm) for SGP CF site area.

AVHRR channel 2 shows stronger angular anisotropy in surface reflectance, while the correction due to atmospheric effects in channel 1 causes larger uncertainty with the Lambertian assumption. More precise classification of surface types would help to improve the BRDF correction and retrieval of surface spectral albedos.

Summary

Surface spectral albedo maps at 1km resolution were derived from AVHRR/NOAA 14 data in channel 1 (0.63 μm) and channel 2 (0.85μm) during the1998-2000 growing seasons over the ARM SGP area (1000 x 1000 km^2) and the North Slope of Alaska/Mackenzie River basin (2500 x 3000km^2). They are available as 1-day and 10-day clear-sky composite products, which may be used for SCM/GCM modelling studies.

BDRF models were derived for various surface types and used for normalization of surface reflectances to common viewing geometry and for the derivation of surface albedo. A model is proposed to account for both the BRDF and topography effects. A sensitivity study showed improved quality of images with a smoother distribution in the surface albedo maps due to a correction for the effect of an inclined surface.

A model study at the SGP CF site shows that neglecting BRDF properties in the satellite retrieval of surface albedo generally leads to relative errors less than 5%. Uncertainty becomes larger (up to 15% to 20%) for SZA and VZA > 60° and more turbid aerosol conditions.

References

Hay, J. E., 1985: Estimating solar irradiance on inclined surfaces: A review and assessment of methodologies. *Int. J. Solar Energy*, **3**, 203-240.

Henderson-Sellers, A., Z.-L. Zhang, and R. E. Dickinson, 1993: The project for intercomparison of land-surface parameterization schemes. *Bull. Amer. Meteorol. Soc*., **74**, 1335-1349.

Iqball, M., 1983: An introduction to solar radiation. *Academic Press*. 390pp.

Kondatyev, K. Ya, 1977: Radiation regime of inclined surfaces. Tech. Note No. 152. WMO-467. Geneva. 82pp.

Lee, T. Y., and Y. J. Kaufman, 1986: Non-Lambertian effects on remote sensing of surface reflectance and vegetation index. *IEEE Trans. Geosci. Remote Sensing*, **24**, 699-708.

Li, Z., J. Cihlar, Z. Zheng, L. Moreau, and H. Ly, 1996: The bidirectional effects of AVHRR measurements over boreal regions. *IEEE Trans. Geosci. Remote Sensing*, **34**, 1308-1322.

Proy, C., D. Tanre, and P. Y. Deschamps, 1989: Evaluation of topographic effects in remotely sensed data. *Rem. Sens. Environ.*, **30**, 21-32.

Rahman, H., and G. Dedieu, 1994: SMAC a simplified method for atmospheric correction of satellite measurements in the solar spectrum. *Int. J. Remote Sens*., **15**, 123-143.

Richter, R., 1998: Correction of satellite imagery over mountainous terrain. *Appl. Optics,* **37**, 4004-4015.

Roujean, J.-L., M. Leroy, and P. Y. Deschamps, 1992: A bidirectional reflectance model of the Earth's surface for the correction of remote sensing data. *J. Geophys. Res.*, **97**, 20,455-20,468.

Stokes, G. M., and S. E. Schwartz, 1994: The Atmospheric Radiation Measurement (ARM) Program: Programmatic background and design of the cloud and radiation test bed. *Bull. Amer. Meteor. Soc*., **75**, 1201-1221.

Stewart, R. E., and Co-authors, 1998: The Mackenzie GEWEX Study: the water and energy cycles of a major North American river basin. *Bull. Amer. Meteor. Soc.,* **79**, 2665-2684.

Vermote, E. F., D. Tanre, J. L. Deuze, M. Herman, and J.-J. Mocrette, 1997a: Second simulation of the satellite signal in the solar spectrum, 6S: An overview. *IEEE Trans. Geosci. Remote Sensing*, **35**, 194-211.

Vermote, E. F., N. E. Saleous, C. O. Justice, Y. F. Kaufman, J. L. Privette, L. Remer, J. C. Roger, and D. Tanre, 1997b: Atmospheric correction of visible to middle infrared EOS-MODIS data over land surfaces: Background, operational algorithm, and validation. *J. Geophys. Res.*, **102**, 17,131-17,141.

Wanner, W., A. H. Strahler, B. Hu, P. Lewis, J.-P. Muller, X. Li, C.L.B. Schaaf, and M. J. Barnsley, 1997: Global retrieval of bidirectional reflectance and albedo over land from EOS MODIS and MISR data: Theory and algorithm. *J. Geophys. Res.*, **102**, 17,143-17,161.